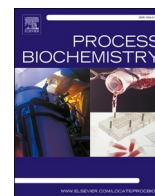




Since January 2020 Elsevier has created a COVID-19 resource centre with free information in English and Mandarin on the novel coronavirus COVID-19. The COVID-19 resource centre is hosted on Elsevier Connect, the company's public news and information website.

Elsevier hereby grants permission to make all its COVID-19-related research that is available on the COVID-19 resource centre - including this research content - immediately available in PubMed Central and other publicly funded repositories, such as the WHO COVID database with rights for unrestricted research re-use and analyses in any form or by any means with acknowledgement of the original source. These permissions are granted for free by Elsevier for as long as the COVID-19 resource centre remains active.



## Clean and folded: Production of active, high quality recombinant human interferon- $\lambda$ 1

Aram Shaldzhyan<sup>a</sup>, Yana Zabrodskaya<sup>a,b,c,\*</sup>, Nikita Yolshin<sup>a</sup>, Tatiana Kudling<sup>d</sup>, Alexey Lozhkov<sup>a,b</sup>, Marina Plotnikova<sup>a</sup>, Edward Ramsay<sup>a</sup>, Aleksandr Taraskin<sup>a,b</sup>, Peter Nekrasov<sup>a</sup>, Mikhail Grudin<sup>a</sup>, Andrey Vasin<sup>a,b</sup>

<sup>a</sup> Smorodintsev Research Institute of Influenza, Russian Ministry of Health, 15/17 Prof. Popov St., St. Petersburg, 197376, Russia

<sup>b</sup> Peter the Great Saint Petersburg Polytechnic University, 29 Polytechnicheskaya, St. Petersburg, 194064, Russia

<sup>c</sup> Petersburg Nuclear Physics Institute named by B. P. Konstantinov of National Research Center "Kurchatov Institute", mkr. Orlova roshcha 1, Gatchina, 188300, Russia

<sup>d</sup> Cancer Gene Therapy Group, Translational Immunology Research Program, University of Helsinki, Helsinki, Finland

### ARTICLE INFO

#### Keywords:

Interferon-lambda  
Immobilized metal affinity chromatography  
Cation exchange chromatography  
Refolding

### ABSTRACT

Type III interferons exhibit antiviral activity against influenza viruses, coronaviruses, rotaviruses, and others. In addition, this type of interferon theoretically has therapeutic advantages, in comparison with type I interferons, due to its ability to activate a narrower group of genes in a relatively small group of target cells. Hence, it can elicit more targeted antiviral or immunomodulatory responses. Obtaining biologically-active interferon lambda (hIFN- $\lambda$ 1) is fraught with difficulties at the stage of expression in soluble form or, in the case of expression in the form of inclusion bodies, at the stage of refolding. In this work, hIFN- $\lambda$ 1 was expressed in the form of inclusion bodies, and a simple, effective refolding method was developed. Efficient and scalable methods for chromatographic purification of recombinant hIFN- $\lambda$ 1 were also developed. High-yield, high-purity product was obtained through optimization of several processes including: recombinant protein expression; metal affinity chromatography; cation exchange chromatography; and an intermediate protein refolding stage. The obtained protein was shown to feature expected specific biological activity in line with published effects: induction of MxA gene expression in A549 cells and antiviral activity against influenza A virus.

### 1. Introduction

Interferons play a critical role in the immune response by suppressing viral spread in the early stages of infection and form the first line of defense against viral infection in mammals [1,2]. According to amino acid sequence and type of receptor through which signal transduction is mediated, interferons are divided into three groups: types I, II, and III [1,3]. Type III interferons (lambda interferons, IFN- $\lambda$ ) are related to type I interferons (interferon- $\alpha$  and interferon- $\beta$ ) and demonstrate a similar antiviral effect [4,5]. Type III interferons are promising therapeutic agents that can induce a more targeted antiviral or immunomodulatory response than other interferon types [6,7]. Such interferons primarily affect viruses that target cells of the respiratory tract, gastrointestinal tract, or liver [8]. Thus, type III interferons exhibit antiviral activity against a number of respiratory and gastrointestinal viruses: influenza

virus; metapneumovirus; respiratory syncytial virus; coronavirus; and rotavirus [6]. Availability of a simple, effective method for producing type III interferons is a necessary prerequisite for further research of its potential as an antiviral or immunomodulatory agent. In previously published work, methods for production of recombinant hIFN- $\lambda$ 1 in soluble form with the proteolytically cleaved S-tag [9], and in the form of inclusion bodies with 6His-tag [5,10], have been proposed.

Brady et al. [11] expressed wild-type and cysteine mutant versions of hIFN- $\lambda$ 1 in *E. coli* in the form of inclusion bodies, followed by refolding by dilution and purification by cation exchange and hydrophobic interaction chromatography. Their method provided a higher yield per liter of culture medium, yet the wild-type hIFN- $\lambda$ 1 thus obtained had several disulfide isomers. Purification methods proposed by Xie et al. [12], Magracheva et al. [13], and Dellgren et al. [5] include a gel filtration step and are thus suitable for small-scale production due to

\* Corresponding author at: Department of Molecular Biology of Viruses, Smorodintsev Research Institute of Influenza, Russian Ministry of Health, 197376, Prof. Popov St. 15/17, St. Petersburg, Russia.

E-mail addresses: [yana@zabrodskaya.net](mailto:yana@zabrodskaya.net), [yana.zabrodskaya@influenza.spb.ru](mailto:yana.zabrodskaya@influenza.spb.ru) (Y. Zabrodskaya).

<https://doi.org/10.1016/j.procbio.2021.08.029>

Received 21 February 2021; Received in revised form 30 August 2021; Accepted 31 August 2021

Available online 2 September 2021

1359-5113/© 2021 Elsevier Ltd. All rights reserved.

limited scalability of the gel filtration method. Li et al. [9] obtained a soluble fusion protein of approximately 77.4 kDa, which contained a Nus-His-S-tag of 57.8 kDa (NusA-S-His-tagged hIFN- $\lambda_1$ ), followed by on-column tag cleavage by thrombin. In this work, we propose a method for expression of hIFN- $\lambda_1$ , bearing an N-terminal 6His-tag and without substitutions in the amino acid sequence of the protein, using a simple refolding procedure and scalable chromatographic purification methods.

The hIFN- $\lambda_1$  produced features specific activity suitable for research and, potentially, future diagnostic or therapeutic application.

## 2. Material and methods

### 2.1. Materials

Reagents obtained from Sigma included: tris base; Na<sub>2</sub>HPO<sub>4</sub>; NaCl; EDTA; PMSF; Tween 20; glycerol; acetonitrile; TFA; trehalose; L-arginine; sodium acetate; acetic acid; HCl; and urea. HisTrap FF Crude and Source 15S 4.6/100 columns were obtained from GE Healthcare; Bio-Scale Mini P6 cartridges and TGX anyKD precast SDS-PAGE gels were obtained from Bio-Rad. For endotoxin evaluation, the LAL Chromogenic Endpoint Assay (#HIT302, Hycult Biotech) was used. For enzymatic hydrolyses, trypsin and chymotrypsin (Promega) were used. Matrices for MALDI-TOF mass spectrometry (HCCA) were manufactured by Bruker.

Lambda interferon levels were evaluated by human IL-29/IL-28B (IFN-lambda 1/3) DuoSet ELISA (DY1598B, R&D Systems, USA). Biological activity experiments were performed using: the A549 cell line (ATCC, CCL-185); F12 K media, fetal bovine serum, and DPBS manufactured by Gibco (USA); and 12-well plates from Thermo Scientific Nunc (USA). Total RNA isolation and real-time PCR were performed using: TRIZol reagent (Invitrogen, USA); M-MLV reverse transcriptase, MMLV Reaction Buffer, and ultrapure water (Promega, USA); BioMaster HS-qPCR (BioLabMix, Russia); and oligo(dT)16 primers (DNA-Synthesis, Russia).

The viral strain A/California/04/09 (H1N1) was obtained from the *Virus and Cell Culture Collection* of the Smorodintsev Research Institute of Influenza (St. Petersburg, Russia). The virus was expanded in chicken embryo. After expansion, purification was carried out by sucrose gradient centrifugation. Viral titer was determined by titration in MDCK cells.

In the graphical abstract the structure 5T5W of hIFN- $\lambda_1$  was used [14].

### 2.2. Plasmid construction

*In silico* optimized sequence (<https://www.genscript.com/tool/s/gensmart-codon-optimization>), encoding hIFN- $\lambda_1$  #Q8IU54 [15], was synthesized by Evrogen and cloned into the pET302/NT-His plasmid. That vector contains a sequence encoding a polyhistidine tag at the N-terminus of synthesized protein. The resultant construct (pET302/NT-His-hIFN- $\lambda_1$ ) was checked for errors by sequencing.

### 2.3. Protein expression

*Escherichia coli* cultures (BL-21 DE3) were transformed with pET302/NT-His-hIFN- $\lambda_1$  and seeded on Luria Bertani (LB) agar plates containing ampicillin (100  $\mu$ g/mL). Individual colonies were picked and grown overnight in LB media (0.5 % yeast extract, 1% Bacto tryptone, 1% NaCl) containing ampicillin. Overnight culture was then used to inoculate fresh LB medium containing ampicillin (OD<sub>600</sub> = 0.1 at start of new incubation). Bacterial cultures were grown in 2 L culture flasks, containing 200 mL of antibiotic-selective LB medium, with agitation (orbital shaker) to an OD<sub>600</sub> value of 0.7. To optimize cultivation conditions, protein expression was induced by various IPTG concentrations (0.5, 0.1, 0.01 mM), and cultures were incubated further (orbital shaker,

32 °C or 37 °C, 3 h). Cultures were sonicated (MSE ultrasonic disintegrator) on ice (10 pulses, of 10 s each, in 30-second intervals), followed by centrifugation for 1 h (20,000 g at +4 °C). Supernatants and pellets were collected separately. Levels of hIFN- $\lambda_1$  expression, and its presence in supernatants or pellets (inclusion bodies), were determined by polyacrylamide gel electrophoresis (SDS-PAGE).

### 2.4. Protein purification and refolding

Chromatographic purification was performed on a GE Healthcare AKTA pure 25 M system. Primary purification of hIFN- $\lambda_1$  was performed by immobilized metal affinity chromatography (IMAC) under denaturing conditions. Cells were centrifuged for 10 min at 4500 g (+4 °C). Next, cell pellets (1 g wet weight) were resuspended in 30 mL of denaturing buffer (20 mM sodium phosphate, 300 mM sodium chloride, 8 M urea, 20 mM imidazole, pH 7.8, 1 mM PMSF); suspensions were sonicated (MSE ultrasonic disintegrator) using 10 pulses (30 s each, at 2 min intervals) on ice. Lysate was clarified by centrifugation for 20 min at 13,000g (+10 °C).

A 1 mL HisTrap FF Crude column was equilibrated with 5 mL of binding buffer (30 mM sodium phosphate, 300 mM sodium chloride, 8 M urea, 20 mM imidazole, pH 7.8) at a flow rate 0.5 mL/min. Clarified lysate was loaded onto the column (at a flow rate of 0.2 mL/min), followed by washing with 20 mL of binding buffer. The target protein was eluted with 5 mL of elution buffer (30 mM sodium phosphate, 300 mM sodium chloride, 8 M urea, 500 mM imidazole, pH 7.8) at a flow rate of 0.2 mL/min. Eluate was monitored by optical density (280 nm wavelength), and fractions of the target protein with an OD<sub>280</sub> greater than 300 mAU were collected. EDTA (0.5 M) was added to target protein fractions to a final concentration of 5 mM. Protein concentration was determined by chromatogram integration using Unicorn 6 software, assuming: the absorbance of a 0.1 % hIFN- $\lambda_1$  solution at 280 nm to be 0.85 per cm of optical path (calculated based on primary protein sequence using the ProtParam service).

Protein refolding was performed by the dilution method. Chilled refolding solution was placed on a magnetic stirrer, and a solution of denatured protein (2 mg/mL) was added dropwise to a final concentration of 0.1 mg/mL. The resulting solution was stirred for 10 min and then incubated for 24 h at +4 °C. The resulting refolded protein solution was filtered through a PES syringe filter (0.45  $\mu$ m pore size).

Final purification was performed by cation exchange chromatography at +6 °C in a Thermo TSX series refrigerator (Thermo Scientific, USA). A SOURCE™ 15S 4.6/100 column was equilibrated with 8 mL of start buffer (20 mM Tris hydrochloride, 2 mM EDTA, pH 7.5) at a flow rate of 2 mL/min. Next, refolded and filtered protein solution was loaded onto the column, followed by column washing with 10 mL of start buffer (2 mL/min). Target protein was eluted with a linear salt gradient (0–1 M NaCl) in start buffer at a flow rate of 2 mL/min for 15 min. Eluate was monitored by optical density at 280 nm; fractions (0.5 mL) featuring OD<sub>280</sub> values above 25 mAU were collected. Fractions were analyzed by polyacrylamide gel electrophoresis. Fractions containing target protein with minimal impurities were combined. The Bio-Scale Mini P6 Desalting Cartridge (Bio-Rad) was used to transfer into phosphate buffered saline (pH 7.2). Protein concentration was determined by the 'DC Protein Assay' (Bio-Rad, USA), based on the Lowry method. Lysozyme (Sigma, USA) was used as the standard protein to produce the calibration curve.

### 2.5. Product analysis

#### 2.5.1. SDS-PAGE

Purified protein was analyzed by SDS-PAGE using the Laemmli method under reducing conditions (with  $\beta$ -mercaptoethanol) and non-reducing conditions (without  $\beta$ -mercaptoethanol) [16]. Electrophoresis materials used (Bio-Rad) included: 'Any kD TGX' precast gels; Kaleidoscope Plus Protein Ladder; PowerPac Basic DC power source; and Mini

Protean Tetra cell. Gels were stained with a Coomassie solution as described [17]. Gels were visualized using the ChemiDoc MP gel documentation system and analyzed using Bio-Rad Image Lab Software.

### 2.5.2. Gel-filtration

Gel filtration analytical chromatography (GF) was performed on a Superdex 200 Increase 10/300 G L column (10 × 300 mm, GE Healthcare) with the Akta Pure 25 chromatographic system (GE Healthcare). Samples were diluted in phosphate-buffered saline to a final protein concentration of 0.1 mg/mL. The chromatographic column was washed with 50 mL of PBS at a flow rate of 1 mL/min. A mixture of standard proteins (ferritin – 440 kDa, ovalbumin – 44 kDa, ribonuclease A – 13.7 kDa and aprotinin – 6.5 kDa), from the GE Gel Filtration Calibration Kit HMW and GE Gel Filtration Calibration Kit LMW, was used for column calibration. Injection volume was 50 µL for standard mix and sample. Elution was performed with phosphate-buffered saline at 1 mL/min at ambient temperature. Elution volume was 35 mL. The chromatogram was recorded at a wavelength of 280 nm. Based on the chromatogram of the standard (protein mixture), a calibration curve was fit, and the molecular weights of peaks were calculated.

### 2.5.3. Enzyme-linked immunosorbent assay

ELISA was carried out using commercial reagents. Levels of hIFN-λ<sub>1</sub> were evaluated by human IL-29/IL-28B (IFN-lambda 1/3) DuoSet ELISA (DY1598B, R&D Systems, USA), according to manufacturer's instructions. A different commercial kit, Mouse IL-28 A/B (IFN-lambda 2/3) DuoSet ELISA (DY1789B, R&D Systems), was used to assess cross-reactivity.

### 2.5.4. MALDI-TOF

The amino acid sequence of recombinant 6xHis-hIFN-λ<sub>1</sub> protein was confirmed using MALDI-TOF mass spectrometry. Following PAGE, fragments were excised from gel and washed twice for dye removal (30 mM NH<sub>4</sub>HCO<sub>3</sub> in 40 % acetonitrile). Gel fragments were next dehydrated with 100 % acetonitrile, dried in air, and subjected to enzymatic digestion by trypsin or chymotrypsin. Trypsin (20 µg/mL in 50 mM NH<sub>4</sub>HCO<sub>3</sub>) was added to gel, and incubation was performed for 2 h at 60 °C. Incubations with chymotrypsin (20 µg/mL in 100 mM Tris-HCl, 1 mM CaCl<sub>2</sub>, pH 8.0) were performed for 18 h at 25 °C. In both cases, reactions were stopped with 1% TFA in 10 % acetonitrile. Peptides after enzymatic digestion were mixed with HCCA matrix, put onto the metal target, and their mass spectra recorded in positive ion registration reflective mode using the UltrafleXtreme MALDI-TOF mass spectrometer (Bruker). Spectra were processed in flexAnalysis software (Bruker). Protein identification was performed in BioTools (Bruker) using MASCOT (<http://www.matrixscience.com/>). It should be noted that recombinant protein amino acid sequence (Fig. 1b) was added to the

local database; during the identification process, the two databases (local and SwissProt, <https://www.uniprot.org/>) were used simultaneously. Mass tolerance was established as 20 ppm; oxidation of methionine was indicated as a variable modification. Identification was considered reliable based on spectrum score and threshold ( $p < 0.05$ ).

## 2.6. Biological activity

Type I and type III interferons induce the expression of ISGs (interferon stimulated genes) through their heterodimeric receptors. One of the key antiviral ISGs is MxA [3]. Unlike most ISGs, the Mx genes are not characterized by constitutive expression; their expression is specifically caused by the action of type I and III IFNs. This makes MxA an excellent marker of activation of an IFN-dependent response [18]. Thus, biologically active hIFN-λ<sub>1</sub> should induce MxA expression. To determine changes in MxA mRNA level, real-time qPCR analysis was performed following sample preparation (RNA isolation, reverse transcription). The antiviral effect of hIFN-λ<sub>1</sub> was shown in A549 cells infected with influenza A virus A/California/04/09 (H1N1).

### 2.6.1. Cell treatment

A549 (carcinomatous alveolar basal epithelial cell line) cells were used. Cells were cultured using: F12 K media with 1% GlutaMax and 10 % fetal bovine serum; and 12-well plates (5 × 10<sup>5</sup> cells/well). Monolayers were washed with DPBS and treated with 10 ng/mL hIFN-λ<sub>1</sub>. After 10 h or 24 h of incubation (37 °C, 5% CO<sub>2</sub>, humidification), hIFN-λ<sub>1</sub> was removed. Cell monolayers were washed again with DPBS. The treated cell cultures and non-treated controls were harvested.

### 2.6.2. RNA isolation

Total RNA was isolated from A549 cells using TRIzol reagent according to manufacturer's instructions. RNA concentration and general integrity were measured using a NanoDrop ND-1000 spectrophotometer (NanoDrop Technologies, USA).

### 2.6.3. Reverse transcription reaction

Following RNA extraction, samples were reverse transcribed using M-MLV reverse transcriptase (M-MLV RT) as described [19]. A mixture of 2 µg total RNA and 1 µg oligo(dT)<sub>16</sub> primers, adjusted with ultrapure water to a final volume of 12 µL, was incubated at 70 °C for 5 min. Tubes were immediately cooled on ice, and a mix was then added containing: 5 µL 5x MMLV Reaction Buffer; 1.5 µL 5 mM dNTPs; 1 µL M-MLV RT; and 5.5 µL ultrapure water. Complementary DNA synthesis was carried out at 42 °C for 60 min. Enzyme (M-MLV RT) was inactivated by heating (65 °C, 5 min). Products were stored at –20 °C.

### 2.6.4. Real-time qPCR

Real-time qPCR assays were performed using the CFX96 Real-Time PCR System (Bio-Rad). Reaction mixtures contained: 12.5 µL of 2x BioMaster HS-qPCR; 0.5 µL (0.6 µM) of each primer and probe; 2 µL of first-strand cDNA; and 9 µL of ultrapure water. Amplification was performed using the following conditions: an activation step (95 °C, 5 min); and 40 cycles of amplification (95 °C for 15 s; 60 °C for 60 s). Fluorescence detection was performed in each cycle at the 60 °C step. The comparative cycle threshold method (ΔΔCT) was used to quantitate MxA expression. Results were normalized to GAPDH endogenous reference expression levels. At least three biological replicates were used for each data point. Statistical analyses were performed using GraphPad Prism 6.0.

### 2.6.5. Antiviral activity

A549 cells were seeded onto 96-well plates (16,000 cells in 100 µL per well). Monolayers were washed with DPBS (Gibco, USA) and treated with hIFN-λ<sub>1</sub> in concentrations from 10 to 240 ng/mL. After 24 h of incubation (37 °C, 5% CO<sub>2</sub> with humidification), hIFN-λ<sub>1</sub> was removed. Cell monolayers were washed again with DPBS and infected with

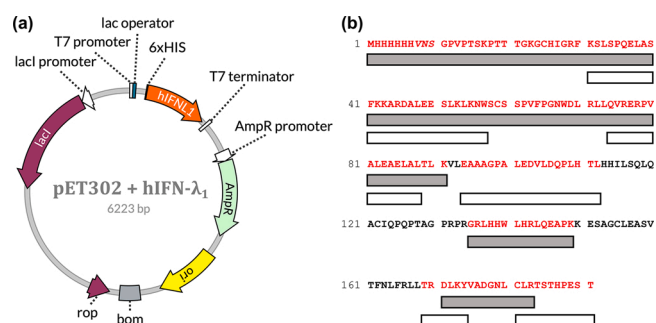


**Fig. 1. Recombinant hIFN-λ<sub>1</sub> protein construction.** (a) Specifics of the pET302+ hIFN-λ<sub>1</sub> expression plasmid. (b) Amino acid sequence of the 6xHis-hIFN-λ<sub>1</sub> recombinant protein. Additional aa residues between the polyhistidine tag and hIFN-λ<sub>1</sub> are indicated in italics. Sequence regions identified using mass spectrometry (Section 3.4.1) are highlighted: black bars and white bars indicate enzymatic digestion with trypsin or chymotrypsin, respectively.

influenza A virus, strain A/California/04/09 (H1N1). For infection, a 100  $\mu$ l volume was used. After 60 min of adsorption at 37 °C, virus was removed, 200  $\mu$ l of fresh medium was added, and the culture incubated at 37 °C (5% CO<sub>2</sub> with humidification). Infected cell cultures and non-infected controls were harvested at 72 h after viral inoculation. Viral loads were evaluated by ELISA using in-house antibodies, as described [20].

### 3. Results and discussion

#### 3.1. Plasmid construction

An *in silico* optimized (<http://genomes.urv.es/OPTIMIZER/optimzed.php>) sequence encoding hIFN- $\lambda_1$  was synthesized and cloned into pET302/NT-His plasmid by Evrogen. The resultant plasmid was verified by sequencing and found to contain no errors. The pET302/NT-His vector contains sequence encoding a 6-histidine tag at the N-terminus of recombinant protein. The features of the expression plasmid are shown in Fig. 1a. The resultant recombinant protein amino acid sequence, encoded by the construct (plasmid pET302/NT-His + hIFN- $\lambda_1$ ), is shown in Fig. 1b.

#### 3.2. Protein expression

Upon IPTG induction, a BL-21 DE3 cell culture transformed with the pET302/NT-His-hIFN- $\lambda_1$  plasmid showed expression of a protein with a molecular weight of about 21 kDa. The theoretical molecular weight of the protein was 21.2 kDa. In the experiment, the concentration of inducer and the incubation temperature were varied. The incubation time with the inducer was 3 h. Each sample was fractionated (Fig. 2a).

Under the conditions tested, the target protein was expressed in the form of inclusion bodies. According to the literature [5,10,21], this is a common occurrence with production of recombinant interferons in *E. coli*. It should be noted that the hIFN- $\lambda_1$  gene was also cloned into the pET22b + vector, at the MscI and XhoI sites, in order to create a fusion protein not only with a histidine tag at the C-terminus, but also with pelB sequence at the N-terminus. The pelB sequence encodes a signal peptide, potentially contributing to periplasmic protein localization. However, even in the presence of the signal peptide, recombinant protein was localized in inclusion bodies (data not shown).

Since cultivation conditions and the presence of pelB sequence did not increase the amount of soluble protein, production of hIFN- $\lambda_1$  was carried out using: pET302/NT-His plasmid; LB medium with ampicillin (100  $\mu$ g/mL); 37 °C incubation; and platform agitation (250 rpm). When the OD<sub>600</sub> value reached 0.7, protein expression was induced by adding IPTG to a final concentration 0.01 mM, and cultivation with induction

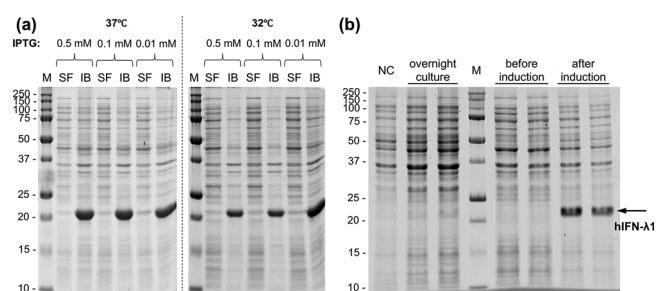


**Fig. 2. Electrophoresis of lysate fractions from the hIFN- $\lambda_1$  producing strain (*E. coli* BL-21).** (a) Induction testing. IPTG concentrations used for induction are highlighted (0.5 mM, 0.1 mM, 0.01 mM). Incubation temperatures are shown (left 37°C, right 32°C). SF – soluble fraction; IB – inclusion bodies. (b) Protein production. 'Overnight culture' - overnight culture, subcultured for production; 'Before induction' - cell lysate before addition of inducer; and 'After induction' - cell lysate, 3 h after addition of inducer. NC – negative control (*E. coli* BL-21 without plasmid).

was continued for 3 more hours (Fig. 2b). We have shown that expression of the protein initially occurs in the form of inclusion bodies, and thus problems with transition of the protein into an insoluble form during prolonged induction should not occur. Also, expression in the form of inclusion bodies, according to the available literature, at least partially protects the product from proteolytic degradation, and the host cells from possible toxicity of the product. Based on this, we decided to implement overnight induction to increase product yield.

#### 3.3. Protein purification and refolding

Primary protein purification was carried out by metal affinity chromatography under denaturing conditions. This purification method, with on-column refolding of hIFN- $\lambda_1$  described earlier [10], showed low yield of refolded protein (less than 5 mg of correctly-folded protein per liter of culture). Therefore, it was decided to perform the first purification step under denaturing conditions, followed by refolding of the partially purified protein. Ni-Sepharose 6 F F resin (prepacked HisTrap FF Crude columns) was chosen because of its high dynamic binding capacity (about 35 mg of hIFN- $\lambda_1$  per 1 mL of sorbent) and the possibility of further scale-up. The chromatogram of the first purification step is shown in Fig. 3a.

Two refolding buffers with different pH (Tris-HCl, pH 7.5; sodium acetate, pH 5.5), with and without refolding additives, were selected for screening. We used buffer systems, which have previously been shown to be effective (in our laboratory experience with recombinant proteins), as starting buffers for refolding. Arginine, glycerol, trehalose, and the non-ionic detergent Tween-20 are common agents used to protect

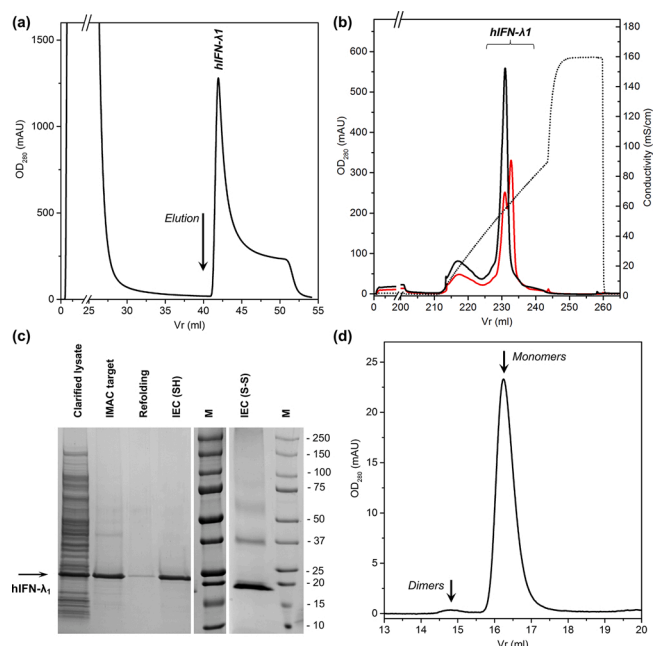


**Fig. 3. Purification stages of hIFN- $\lambda_1$ .** (a) Primary purification of recombinant hIFN- $\lambda_1$  by IMAC. Solid line: absorbance at 280 nm; the initial point of elution is marked with arrow. (b) Final purification of recombinant hIFN- $\lambda_1$  by cation exchange chromatography at room temperature (solid red line) and at +6 °C (solid black line). Solid lines indicate absorbance at 280 nm (left y-axis); dashed line indicates conductivity of the solution (right y-axis). (c) PAGE of 6His-hIFN- $\lambda_1$ -containing samples at various stages. Key: M – marker (Precision Plus mol. weight standard); 'IMAC target' – target peak from metal-affinity column; 'Refolding' – material after refolding; 'IEC' – material after cation exchange chromatography (final stage); 'SH' – reducing PAGE conditions (with  $\beta$ -mercaptoethanol); 'S-S' – non-reducing conditions (without  $\beta$ -mercaptoethanol). Coomassie staining. (d) Gel filtration analytical chromatography of recombinant hIFN- $\lambda_1$ . Solid line: absorbance at 280 nm. Peaks corresponding to hIFN- $\lambda_1$  monomers (~98 %) and dimers (<1.5 %) are marked with arrows.

protein from surface-induced aggregation during refolding. Two pH values were chosen because the ProtParam software does not take protein folding into account when calculating the isoelectric point.

Denatured recombinant protein samples (at a concentration of 2 mg/mL) were added to pre-cooled refolding buffer (to final concentration of 100 µg/mL) and mixed by pipetting, followed by incubation for 24 h at +4 °C. Precipitated protein was removed by centrifugation for 1 h at 20,000g. Supernatants were collected and dialyzed against phosphate buffered saline for 24 h, followed by filtration through a PES syringe filter (0.2 µm pore size). Protein concentrations were determined by the Lowry method. For estimation of relative 'soluble protein yield' of refolding variations, 100 µg/mL was designated as 100 %. The results of the experiment are shown in Table 1.

The highest yields of recombinant hIFN-λ<sub>1</sub> in soluble form were seen with two specific refolding buffers: Buffer C (80 %); and Buffer E (89 %). The proposed refolding method provides a significantly higher yield, takes less time, and is more economical in comparison with the stepwise dialysis method proposed [5] for IFN-λ<sub>3</sub>, another type III interferon. Conductivity of the protein solution after refolding was about 5 mS/cm; therefore, it does not interfere with subsequent ion-exchange chromatography. There is thus no need for dialysis or diafiltration of the refolded protein solution. It is possible to proceed directly to the final purification step.

The isoelectric point of the hIFN-λ<sub>1</sub> recombinant protein was 9.08 according to the ProtParam Tool [22]. Thus, hIFN-λ<sub>1</sub> in refolding solution is positively charged, so cation exchange chromatography was chosen as a final purification step. With comparison of different cation exchange resins, the best results (maximum protein yield, minimal impurities) were noted (data not shown) with resins featuring particle size of 15 µm or less, such as Source 15S (GE Healthcare) and ENrich S (Bio-Rad). Source 15S was selected because of higher flow rates and availability for purchase in bulk (for potential process scale-up later). The chromatogram of the final protein purification step is shown in Fig. 3b. The target protein eluted in the conductivity range from 45 to 65 mS/cm. It should be noted that hIFN-λ<sub>1</sub>, at room temperature, elutes as a double peak (Fig. 3b, solid red line). This may indicate the presence of two different conformational variants or a simultaneous presence of monomer/dimer combinations. When elution was performed at +6 °C, a single peak of recombinant protein resulted (Fig. 3b, solid black line); this very likely indicates the presence of a single conformational variant in the sample.

The associated mass and yield values, for all purification and refolding steps, are presented in Table 2. The method makes it possible to obtain up to 70 mg of recombinant hIFN-λ<sub>1</sub> from 1 L of cell culture (~5.2 g wet weight). Expression in the form of inclusion bodies protects the protein from proteolysis during cultivation. Simple and effective refolding provides a high yield of native-form protein with proven biological activity (sec. 3.5).

In order to compare the purification and refolding process developed here with methods described in the literature, we collected known data in Table 3. Despite our significantly lower protein yield, in comparison with the method proposed by Brady et al. in 2004 [11], our method provides a single protein isoform if purification is maintained at +6 °C during cation exchange chromatography. Among the advantages of our method is the use of scalable chromatographic purification methods

**Table 1**  
Soluble protein yield in various refolding buffers.

Refolding Buffer	Soluble Protein Yield, %
(A) 20 MM tris-HCl, pH 7.5	42
(B) 20 MM tris-HCl, 1 M L-arginine, pH 7.5	55
(C) 20 MM tris-HCl, 20 % glycerol, pH 7.5	80
(D) 20 MM tris-HCl, 5% trehalose, pH 7.5	40
(E) 20 MM tris-HCl, 0.1 % Tween-20, pH 7.5	89
(F) 10 MM sodium acetate, pH 5.5	15
(G) 10 MM sodium acetate, 5% trehalose, pH 5.5	12

**Table 2**  
Summary of all purification steps in physical values.

Step	Total protein <sup>b</sup> (mg)	Volume (ml)	Concentration (mg/mL)	Purity <sup>c</sup> (%)	Yield <sup>d</sup> (%)
Cell lysate <sup>a</sup>	370.0	32.0	11.6	4.9	(100.0)
IMAC elution	18.1	10.0	1.8	91.6	91.4
Refolded solution	16.2	200.0	0.1	91.1	81.4
CEX peak	11.9	8.0	1.5	100.0	65.6

<sup>a</sup> From 1 g wet weight pellet.

<sup>b</sup> Determined by Lowry method using lysozyme as standard protein.

<sup>c</sup> Based on SDS-PAGE.

<sup>d</sup> Yield was determined based on total protein measurement (Lowry method) and densitometry of the target PAGE band; the amount of the target protein in cell lysate was designated as 100 %.

(affinity and ion exchange chromatography), in comparison with the methods proposed in [5,12,13] (gel filtration has scale-up limitations). Further, we were unable to achieve reproducible results when using the on-column refolding method proposed in [10].

### 3.4. Product analysis

#### 3.4.1. SDS-PAGE, GF, and MALDI-TOF

The purity of the recombinant protein was analyzed by SDS-PAGE. Fig. 3c shows all steps of target protein purification. The presence of a band with an electrophoretic mobility of about 21 kDa (indicated by an arrow) indicates selective isolation of the protein from the protein mixture present in the cell culture. It should be noted that under non-reducing conditions (Fig. 3c, 'IEC S-S'), a minor band (near the 37 kDa reference), likely representing dimers, is seen. This could be interpreted as a sample preparation artifact. Gel-filtration results indicate a predominance of the main form (mol. weight ~ 25 kDa, corresponding to hIFN-λ<sub>1</sub> monomer), with the dimeric form associated fraction constituting less than 1.5 %. Thus, it can be concluded that the resultant protein product consists predominantly of the monomeric hIFN-λ<sub>1</sub> form (~ 98 %).

Confirmation of recombinant protein amino acid sequence was carried out using MALDI-TOF mass spectrometry after enzymatic hydrolysis of 'protein in gel' with trypsin. In the area marked with an arrow (Fig. 3c), the 6xHis-hIFN-λ<sub>1</sub> recombinant protein was reliably identified (Score/threshold was 156/76, sequence coverage 70 %). Additional hydrolysis with chymotrypsin extends the sequence coverage to 85 %. Protein sequences found in mass spectra are highlighted in Fig. 1b. The registered ions and the corresponding peptides are presented in Table S1. Thus, the obtained protein was reliably identified as human interferon lambda-1 (6xHis-hIFN-λ<sub>1</sub>).

#### 3.4.2. ELISA

Binding of the recombinant protein with anti-hIFNλ<sub>1</sub> monoclonal antibodies was shown by sandwich ELISA. The commercial 'Human IL-29/IL-28B (IFN-lambda 1/3) DuoSet ELISA' kit (DY1598B, R&D Systems) was used (Fig. 4).

For each concentration, the average optical absorbance (OD<sub>450</sub>-OD<sub>655</sub>) is indicated in relative units. Concentrations of hIFN-λ<sub>1</sub> were determined by the Lowry method. These results show that a constant +4 °C temperature is the preferred storage condition for recombinant hIFN-λ<sub>1</sub> protein, not -80 °C followed by thawing. Increasing the stability of the protein product is a priority goal for further improvement of this method. Ideally, this would minimize changes associated with one or more 'freeze-thaw' cycles.

**Table 3**

Comparison between the developed purification method and others proposed in the literature. Advantages are highlighted in green [5,9–13,30].

Source	Isoforms	Purification process	Expression system	Endotoxin level	Yield, mg/L medium
Shaldzhyan et al. (the method developed)	One peak (if CEX carried out at +6°C)	Metal-affinity and cation exchange chromatography used - good scalability	E. coli	0.05 EU/μg	70
Brady et al. 2004 [11]	Two peaks (disulfide isoforms)	Cation exchange and hydrophobic chromatography - good scalability	E. coli	---	200
Xie et al., 2007 [12]	---	Gel filtration on Superdex used during purification process - scalability not ideal	P. pastoris	---	---
Magracheva et al., 2010 [13]	---	Gel filtration on Superdex used during purification process - scalability not ideal	Insect cells	---	---
Meager et al., 2014 [30]	---	---	NS0 cells (mammalian cells)	"A low level of endotoxin was detected in the preparations"	65
Li et al., 2007 [10]	---	Metal-affinity with on-column refolding (did not work in our case)	E. coli	---	86
Li et al., 2006 [9]	---	Affinity with tag removal	E. coli	---	60
Dellgren et al., 2009 [5]	Dimeric form observed	Metal-affinity, cation exchange and gel filtration on Superdex	E. coli	"We could not detect any endotoxins (data not shown), although it should be noted that the E-TOXATE kit only gives a semiquantitative answer"	15

### 3.5. Confirmation of biological activity

#### 3.5.1. *Limulus ameobocyte lysate testing*

In order to exclude the possibility of stimulation of A549 cells by bacterial lipopolysaccharides, the endotoxin level was determined by LAL test. The results show that recombinant hIFN-λ<sub>1</sub> solution contains endotoxin at a concentration of about 25 EU/mL, which corresponds to no more than 5 ng/mL of endotoxin [23]. The concentration of the analyzed sample was 620 μg/mL. Consequently, there was less than 0.05 EU endotoxin per μg of protein, which is in line with commercial analogues on the market [24]. Thus, endotoxins present in the solution should not significantly affect the immune response of cells. Moreover, it has been shown that lipopolysaccharides do not induce the production of either IFN-α/β or IFN-λ in respiratory epithelial cells [18,25]. The A549 cells used here are also a respiratory epithelial line, and lipopolysaccharide-induced MxA expression is not expected.

#### 3.5.2. *Activation of an IFN-dependent response*

The biological activity of hIFN-λ<sub>1</sub> was shown by RT-PCR. Increased MxA expression was shown in A549 cells treated for 10 h with hIFN-λ<sub>1</sub> (10 ng/mL) compared to control cells (Fig. 5a). The level of MxA expression increased by more than 20-fold. Since MxA is an interferon-stimulated gene, increased expression can be considered reliable evidence of the biological activity of the obtained hIFN-λ<sub>1</sub> [18]. Such an approach was also demonstrated [21]. It was shown that MxA is more inducible, in response to the action of hIFN-λ<sub>1</sub>, than oligoadenylate synthase (OAS), another canonical antiviral IGS.

#### 3.5.3. *Evaluation of antiviral activity*

The antiviral effect of IFN-λ has been shown in relation to various influenza A virus types [1,7,26,27]. The action of IFN-λ<sub>1</sub> leads to expression of a wide group of ISGs, which include such antiviral genes as MxA, OAS, and IFITM1 [28]. Thus, to confirm IFN-λ<sub>1</sub> biological activity, the ability to suppress influenza A virus replication was assessed. Administration of exogenous IFN-λ<sub>1</sub> led to a decrease in viral

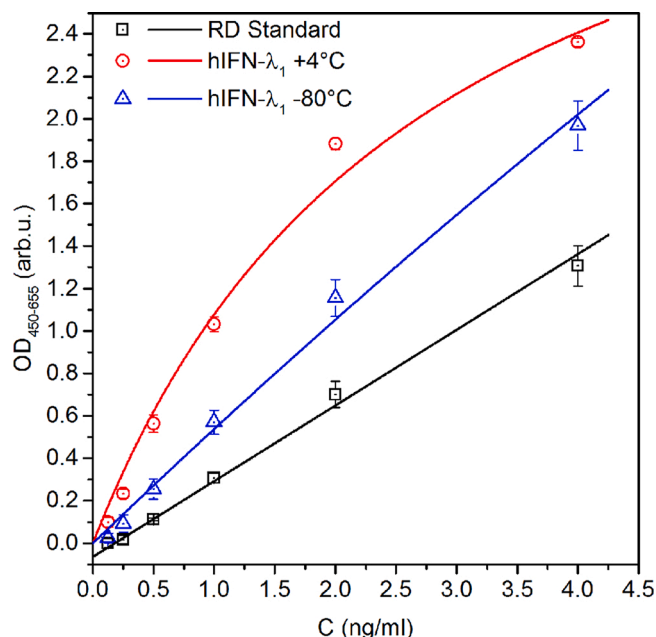


**Fig. 4.** Comparison of ELISA signal from recombinant hIFN- $\lambda_1$  stored in different conditions. In addition to the two storage conditions (+4 °C and -80 °C), a commercial standard is shown from the 'Human IL-29/IL-28B kit (IFN-lambda 1/3) DuoSet' ELISA kit (DY1598B, R&D Systems).

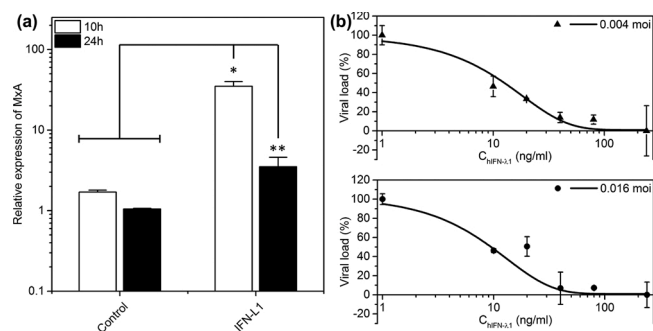


**Fig. 5.** Biological activity of recombinant hIFN- $\lambda_1$ . (a) Change in MxA expression in A549 cells treated with hIFN- $\lambda_1$  (10 ng/mL) for 10 or 24 h during incubation. The y-axis shows relative MxA expression; the x-axis shows cell treatment conditions. The differences in MxA-2 mRNA expression between the control group at 10 h and the control group at 24 h were insignificant ( $p = 0.3333$ ). T-test was performed using the nonparametric Mann-Whitney test. \*  $p$ -value = 0.0286; \*\*  $p$ -value = 0.0159. (b)  $EC_{50}$  determination (hIFN- $\lambda_1$  and influenza virus A/California/04/09 (H1N1)). The y-axes show the relative level of influenza nucleoprotein (100 % corresponds to the NP concentration in infected cells without hIFN- $\lambda_1$  pretreatment). The x-axes show hIFN- $\lambda_1$  concentration (ng/mL). The approximation was performed using a dose-response relationship with  $R^2$  values of 0.97 and 0.98, for 0.004 moi and 0.016 moi, respectively.

nucleoprotein levels in A549 cell supernatants (Fig. 5b). We determined the concentration of interferon at which there was a two-fold decrease in viral load ( $EC_{50}$ ). At infectious doses of 0.004 moi and 0.016 moi,  $EC_{50}$  values were  $(11.0 \pm 1.0)$  ng/mL and  $(9.1 \pm 0.8)$  ng/mL, respectively ( $p = 0.05$ ). Thus, close  $EC_{50}$  values were obtained for different infectious doses.

It should be noted that another group [21] also assessed the ability of recombinant IFN- $\lambda_1$ , and its synthetic analogs, to inhibit influenza A virus (H3N2 subtype) replication. The  $EC_{50}$  value for IFN- $\lambda_1$  was about 1 ng/mL. The differences in  $EC_{50}$  values can be explained by the fact that susceptibility to interferon action varies significantly, depending on the

subtype and strain of influenza A virus [29]. On the other hand, it is possible that not all IFN- $\lambda_1$  molecules have the correct folding, and a certain fraction of the molecules may not have biological activity. However, the fact that a single product peak is observed on the chromatogram (Fig. 3b) indicates the presence of one isoform of the recombinant hIFN- $\lambda_1$  in the sample.

#### 4. Conclusion

The methods for producing recombinant hIFN- $\lambda_1$  proposed earlier in publications have several of disadvantages: the presence of substitutions in the amino acid sequence of the protein; unspecified endotoxin content in the final product; the use of poorly scalable chromatographic methods; non-reproducible refolding methods; and the use of large fusion tags cleaved by thrombin or other enzymes of animal origin. The method developed here provides combination of: sufficiently high protein yield (up to 70 mg/L medium); low endotoxin level (0.05 EU/ug); uniformity of the obtained product in terms of conformation; biological activity of the protein comparable to the literature; and the potential for scaling up the proposed technique without the need for significant changes in terms of purification or refolding, which are critical steps in the production of this protein.

It is therefore potentially suitable for isolation of type III interferons not only for research and diagnostic applications, but also for therapeutic use.

#### Author contributions

Contributions were as follows: A.S. — methodology, data collection, data analysis, writing of manuscript; A.L., N.Y., M.P. — data collection, data analysis, writing of manuscript; T.K., A.T., P.N. — data collection, data analysis; Y.Z. — data collection, data analysis, writing of manuscript, visualization; E.R. — writing, review and editing of manuscript; M.G., A.V. — resources, supervision.

#### Declaration of Competing Interest

The authors report no declarations of interest.

#### Acknowledgment

This work was supported by a Russian State Assignment for fundamental research (0784-2020-0023).

#### Appendix A. Supplementary data

Supplementary material related to this article can be found, in the online version, at doi:<https://doi.org/10.1016/j.procbio.2021.08.029>.

#### References

- [1] M.J. Killip, E. Fodor, R.E. Randall, Influenza virus activation of the interferon system, *Virus Res.* 209 (2015) 11–22, <https://doi.org/10.1016/j.virusres.2015.02.003>.
- [2] M.D.R. Baños-Lara, L. Harvey, A. Mendoza, D. Simms, V.N. Chouljenko, N. Wakamatsu, K.G. Kousoulas, A. Guerrero-Plata, Impact and regulation of lambda interferon response in human metapneumovirus infection, *J. Virol.* 89 (2015) 730–742, <https://doi.org/10.1128/JVI.02897-14>.
- [3] R.E. Randall, S. Goodbourn, Interferons and viruses: an interplay between induction, signalling, antiviral responses and virus countermeasures, *J. Gen. Virol.* 89 (2008) 1–47, <https://doi.org/10.1099/vir.0.83391-0>.
- [4] M.R. Thompson, J.J. Kaminski, E.A. Kurt-Jones, K.A. Fitzgerald, Pattern recognition receptors and the innate immune response to viral infection, *Viruses* 3 (2011) 920–940, <https://doi.org/10.3390/v3060920>.
- [5] C. Dellgren, H.H. Gad, O.J. Hamming, J. Melchjorsen, R. Hartmann, Human interferon- $\lambda_3$  is a potent member of the type III interferon family, *Genes Immun.* 10 (2009) 125–131, <https://doi.org/10.1038/gene.2008.87>.
- [6] P. Hermant, T. Michiels, Interferon- $\lambda$  in the context of viral infections: production, response and therapeutic implications, *J. Innate Immun.* 6 (2014) 563–574, <https://doi.org/10.1159/000360084>.

- [7] S. Davidson, S. Crotta, T.M. McCabe, A. Wack, Pathogenic potential of interferon  $\alpha$  in acute influenza infection, *Nat. Commun.* 5 (2014) 3864, <https://doi.org/10.1038/ncomms4864>.
- [8] H.M. Lazear, T.J. Nice, M.S. Diamond, Interferon- $\lambda$ : immune functions at barrier surfaces and beyond, *Immunity* 43 (2015) 15–28, <https://doi.org/10.1016/j.immuni.2015.07.001>.
- [9] M. Li, S. He, Purification and characterization of recombinant human interleukin-29 expressed in *Escherichia coli*, *J. Biotechnol.* 122 (2006) 334–340, <https://doi.org/10.1016/j.jbiotec.2005.11.019>.
- [10] M. Li, D. Huang, On-column refolding purification and characterization of recombinant human interferon- $\lambda$ 1 produced in *Escherichia coli*, *Protein Expr. Purif.* 53 (2007) 119–123, <https://doi.org/10.1016/j.pep.2006.11.011>.
- [11] L.J. Brady, K.M. Klucher, C. Chan, D.L. Dong, H.Y. Liu, P.O. Sheppard, T. R. Bukowski, Homogeneous Preparations of IL-28 and IL-29 - Patent US-7485701-B2 - PubChem, US-7485701-B2, 2004. <https://pubchem.ncbi.nlm.nih.gov/patent/US7485701>.
- [12] Y.F. Xie, H. Chen, B.R. Huang, Expression, purification and characterization of human IFN- $\lambda$ 1 in *Pichia pastoris*, *J. Biotechnol.* 129 (2007) 472–480, <https://doi.org/10.1016/j.jbiotec.2007.01.018>.
- [13] E. Magracheva, S. Pletnev, S. Kotenko, W. Li, A. Wlodawer, A. Zdanov, Purification, crystallization and preliminary crystallographic studies of the complex of interferon- $\lambda$ 1 with its receptor, *Acta Crystallogr. Sect. F Struct. Biol. Cryst. Commun.* 66 (2010) 61–63, <https://doi.org/10.1107/S1744309109048817>.
- [14] J.L. Mendoza, W.M. Schneider, H.-H. Hoffmann, K. Vercauteren, K.M. Jude, A. Xiong, I. Moraga, T.M. Horton, J.S. Glenn, Y.P. de Jong, C.M. Rice, K.C. Garcia, The IFN- $\lambda$ -IFN- $\lambda$ R1-IL-10R $\beta$  complex reveals structural features underlying type III IFN functional plasticity, *Immunity*. 46 (2017) 379–392, <https://doi.org/10.1016/j.immuni.2017.02.017>.
- [15] IFNL1 - Interferon lambda-1 precursor - Homo sapiens (Human) - IFNL1 gene & protein, (n.d.). <https://www.uniprot.org/uniprot/Q8IU54>. (Accessed 2 December 2020).
- [16] U.K. Laemmli, Cleavage of structural proteins during the assembly of the head of bacteriophage T4, *Nature* 227 (1970) 680–685, <https://doi.org/10.1038/227680a0>.
- [17] A.A. Shaldzhyan, Y.A. Zbrodskaya, I.L. Baranovskaya, M.V. Sergeeva, A. N. Gorshkov, I.I. Savin, S.M. Shishlyannikov, E.S. Ramsay, A.V. Protasov, A. P. Kukhareva, V.V. Egorov, Old dog, new tricks: influenza a virus NS1 and in vitro fibrillogenesis, *BioRxiv* (2020) 188300, <https://doi.org/10.1101/2020.08.17.254060>.
- [18] O. Haller, P. Staeheli, M. Schwemmler, G. Kochs, Mx GTPases, Dynamamin-like antiviral machines of innate immunity, *Trends Microbiol.* 23 (2015) 154–163, <https://doi.org/10.1016/j.tim.2014.12.003>.
- [19] M.A. Plotnikova, S.A. Klotchenko, A.V. Vasin, Development of a multiplex quantitative PCR assay for the analysis of human cytokine gene expression in influenza A virus-infected cells, *J. Immunol. Methods* 430 (2016) 51–55, <https://doi.org/10.1016/j.jim.2016.01.005>.
- [20] M.A. Plotnikova, S.A. Klotchenko, K.I. Lebedev, A.A. Lozhkov, A.S. Taraskin, N. E. Gyulikhandanova, E.S. Ramsay, A.V. Vasin, Antibody microarray immunoassay for screening and differential diagnosis of upper respiratory tract viral pathogens, *J. Immunol. Methods* 478 (2020) 112712, <https://doi.org/10.1016/j.jim.2019.112712>.
- [21] Z. Zou, D. Yu, M. Zhao, L. Dong, L. Zhao, M. Zou, H. Liu, M. Zhang, H. Sun, Design and evaluation of novel interferon lambda analogs with enhanced antiviral activity and improved drug attributes, *Drug Des. Devel. Ther.* 10 (2016) 163, <https://doi.org/10.2147/DDDT.S91455>.
- [22] ExPASy - ProtParam tool, (n.d.). <https://web.expasy.org/protparam/>. (Accessed 1 November 2020).
- [23] Cell Culture FAQs: Bacterial Endotoxin Contamination | Sigma-Aldrich, (n.d.). <https://www.sigmaaldrich.com/technical-documents/articles/biology/what-is-endotoxin.html>. (Accessed 28 November 2020).
- [24] Recombinant Human Interferon lambda-3(IFNL3) (Active) - Cusabio, (n.d.). <https://www.cusabio.com/Interleukin/Recombinant-Human-Interferon-lambda-3-IFNL3-12923581.html>. (Accessed 28 November 2020).
- [25] I. Ioannidis, F. Ye, B. McNally, M. Willette, E. Flano, Toll-like receptor expression and induction of type I and type III interferons in primary airway epithelial cells, *J. Virol.* 87 (2013) 3261–3270, <https://doi.org/10.1128/jvi.01956-12>.
- [26] I.E. Galani, V. Triantafyllia, E.-E. Eleminiadou, O. Koltzida, A. Stavropoulos, M. Manioudaki, D. Thanos, S.E. Doyle, S.V. Kotenko, K. Thanopoulou, E. Andreacos, Interferon- $\lambda$  mediates non-redundant front-line antiviral protection against influenza virus infection without compromising host fitness, *Immunity* 46 (875–890) (2017) e6, <https://doi.org/10.1016/j.immuni.2017.04.025>.
- [27] S.T. Peterson, E.A. Kennedy, P.H. Bringle, G.M. Taylor, K. Urbaneck, T.L. Bricker, S. Lee, H. Shin, T.S. Dermody, A.C.M. Boon, M.T. Baldrige, Disruption of type III interferon (IFN) genes *Ifnl2* and *Ifnl3* recapitulates loss of the type III IFN receptor in the mucosal antiviral response, *J. Virol.* 93 (2019), <https://doi.org/10.1128/JVI.01073-19>.
- [28] A. Egli, D.M. Santer, D. O'Shea, D.L. Tyrrell, M. Houghton, The impact of the interferon-lambda family on the innate and adaptive immune response to viral infections, *Emerg. Microbes Infect.* 3 (2014) 1–12, <https://doi.org/10.1038/emi.2014.51>.
- [29] C. Chaimayo, M. Dunagan, T. Hayashi, N. Santoso, T. Takimoto, Specificity and functional interplay between influenza virus PA-X and NS1 shutoff activity, *PLoS Pathog.* 14 (2018) e1007465, <https://doi.org/10.1371/journal.ppat.1007465>.
- [30] A. Meager, A. Heath, P. Dilger, K. Zoon, M. Wadhwa, Standardization of human IL-29 (IFN- $\lambda$ 1): establishment of a world health organization international reference reagent for IL-29 (IFN- $\lambda$ 1), *J. Interferon Cytokine Res.* 34 (2014) 876–884, <https://doi.org/10.1089/jir.2014.0015>.